STRUCTURE-PROCESS-PROPERTY RELATIONSHIP OF CONDUCTIVE EXFOLIATED GRAPHITE NANOPLATELET / POLYLACTIC ACID FILMS

E. M. Sullivan[a*], Y. J. Oh[b], R. A. Gerhardt[a], B. Wang[a,c], and K. Kalaitzidou[a,b]

[a]*School of Materials Science & Engineering, Georgia Institute of Technology, 771 Ferst Drive, Atlanta, GA 30332-0245, U.S.A.*
[b]*George W. Woodruff School of Mechanical Engineering, Georgia Institute of Technology, 801 Ferst Drive, Atlanta, GA 30332-0405, U.S.A.*
[c]*Georgia Tech Manufacturing Institute, Georgia Institute of Technology, 813 Ferst Drive, Atlanta, GA 30332-0560, U.S.A.*
**erin.sullivan@gatech.edu*

Keywords: Polylactic acid, exfoliated graphite nanoplatelets, crystallinity, electrical conductivity

Abstract
Exfoliated graphite nanoplatelets (GNP) / polylactic acid (PLA) composite films were fabricated using a scalable, melt compounding and compression molding process and the effect of cooling rate on the mechanical, viscoelastic and electrical properties of the composite films was examined. With superior conductivity, GNP enhances PLA, making it a green alternative to current conductive films made of petroleum based polymers for static dissipation applications. The crystallinity and crystal structure was investigated using differential scanning calorimetry (DSC) and wide angle X-ray diffraction (WAXD). Electrical conductivity and tensile properties were also determined as a function of crystallinity/cooling rate. Both the crystallinity and the electrical conductivity increased with decreased cooling rate. It is concluded that for the same material system and processing method the electrical conductivity can be tailored by tuning the processing conditions, such as the cooling rate, during compression molding.

1. Introduction

Thermally and electrically conductive films have many applications for static and thermal dissipation particularly in electronics packaging. Furthermore, conductive polymer composites are currently being investigated due to their low density, as well as their resistance to oxidation and corrosion. Previous research has been conducted investigating various fillers and matrices for such applications. Carbon nanotubes (CNT) and CNT buckypaper (BP) coupled with various thermosetting matrices, such as epoxy [1] and bismaleimide (BMI) [2], have been of particular interest. There are many drawbacks to using CNT and BP as fillers for such applications. The one-dimensional geometry of CNT limits the two-dimensional conductivity in CNT composites. Furthermore, BP is comprised of a dense network of CNT [1, 3], which is desirable for

conductivity in that there are numerous conductive pathways. However, the dense network of CNT is difficult for polymer resins to penetrate and have good interface interactions. In this study, exfoliated graphite nanoplatelets (GNP) were used due to their two-dimensional planar structure. GNP has the same chemistry as CNT and the same conducting properties. However, the intercalated and exfoliated two-dimensional benzene network allows for more conductive pathways, potentially lowering the percolation threshold [1, 4].

One of the primary drawbacks to using a thermosetting resin as a matrix material is that thermosets are not recyclable. In order to achieve good recyclability properties, a thermoplastic polymer must be used. Thermoplastic matrices can offer recyclability, as well as, sufficient mechanical integrity for use in electronics packaging. Biopolymers are of high interest due to their biodegradability and sustainability. Polylactic acid (PLA) is a biodegradable thermoplastic polyester that is derived from sugar or cornstarch [5, 6]. PLA has properties comparable to many petroleum based polymers making it an ideal alternative. This paper focuses on the effect of cooling rate during compression molding on GNP/PLA films' crystallinity and how the resultant crystallinity affects other composite properties, specifically mechanical and electrical.

2. Experimental

2.1 Materials

NatureWorks LLC's (Minnetonka, MN) commercially available semicrystalline PLA pellets (3051D) were used as the matrix material. The PLA pellets have a specific gravity of 1.24 and a flow index of 10-30 g/10min, according to ASTM D1238. Grade C GNP purchased from XG Sciences (East Lansing, MI) was used as the nanomaterial. The GNP has a specific surface area of ~750 m^2/g, an average diameter of approximately 1-2 μm, and a thickness on the order of 10-20 nm.

2.2 Processing

The films were fabricated using a scalable, two-step melt compounding and compression molding manufacturing process. First, the GNP was incorporated into the PLA matrix via melt blending using a DSM 15cc compounder (vertical, co-rotating twin-screw microextruder) at an operating temperature of 190°C and a screw speed of 150 RPM for approximately 3 minutes. The composite melt was then extruded out of the 0.8 mm orifice at a pull-out rate of 15 RPM and spun into fibers of ~60-70 μm in diameter using a drawing speed of ~625 RPM. The fibers were then compression molded into films of ~160 μm thick using a manual four-column 12 ton Carver hydraulic press (model 4122) with heated and water cooled platens. The fibers were placed on the heated platens (180°C) and allowed to soften for 5 minutes. (An aluminum foil mold was used to help the melted fibers retain the desired film shape and thickness.) Then the softened fibers were pressed at a force of ~907 kg (2,000 lbs) for 5 minutes. The films were then cooled at either ~0.4 °C/min without water assisted cooling (referred to as slow cooled, SC) or ~16 °C/min with water assisted cooling (referred to as fast cooled, FC) to investigate the effect of cooling rate on the resultant composite properties. All films were cooled to ~40°C, below the glass transition temperature, prior to being removed from the hot press in order to avoid inducing stress concentrations and plastic deformation. By first producing composite fibers, the GNP

agglomeration size can be minimized. (The maximum agglomeration size in the resultant composite films should not exceed the maximum fiber diameter of ~60-70 μm.)

2.3 Characterization

The morphology and structure of the films was examined using scanning electron microscopy (SEM), Phenom World G2 Pro, at an accelerating voltage of 5kV. The samples were first coated with gold using a Cressington Sputter Coater 108 (model 6002) for enhanced conductivity. Gold was deposited on the sample surfaces at ~0.08 mbar and ~30 mA using a 30 second deposition time.

The crystallinity of the films was examined using differential scanning calorimetry (DSC), TA Instruments DSC Q2000 in standard mode. Samples of 5-7mg were prepared in standard Tzero Al sample pans at 20°C, and held isothermal for 5 minutes. The samples were heated to 175°C at a 5°C/min heating rate, and then cooled to 20°C at a 5°C/min cooling rate. The initial heating cycle was used to calculate crystallinity in order preserve thermal history and investigate the effect of processing on crystallinity. The crystal structure of the films was examined with wide-angle X-ray diffraction (WAXD). Measurements were performed using a X'Pert Pro Alpha 1 (PANalytical, Almelo, Netherlands) diffractometer. (Cu Kα radiation, λ = 1.541Å, 45kV and 40mA) Diffraction patterns were collected from a 2θ angle of 8° to 40° with a step size of ~0.02.

Tensile properties of the films were examined using rectangular samples with a gauge length of 40mm accordance with ASTM D882. An Instron 33R4466 tensile tester and a 10 kN load cell were used.

The electrical properties were determined using impedance spectroscopy [7]. A Solartron 1260 Impedance/Gain Phase Analyzer along with a 1296 Dielectric Interface was used to measure in the 0.1 Hz-10 MHz frequency range.

3. Results

3.1 Morphology

The morphology of the ~160 μm thick films was examined using SEM. Representative images of both the slow and fast cooled samples can be seen in Figure 1. The SEM indicated there are no voids or micro-porosity on the films and very minimal surface defects. The surface defects present on the films were limited to the slight striation pattern seen in Figure 1. The surface striations are a result of the compression molding. The surface of the platens combined with the surface of the aluminum foil mold result in this defect. However, the striations are minimal in comparison to the thickness (~160 μm) and therefore were deemed negligible for the purpose of this study. Small agglomerations of GNP, ~5-10 μm, were also seen in the films containing GNP. These small clusters are depicted in Figure 1a and 1b and indicated with an arrow.

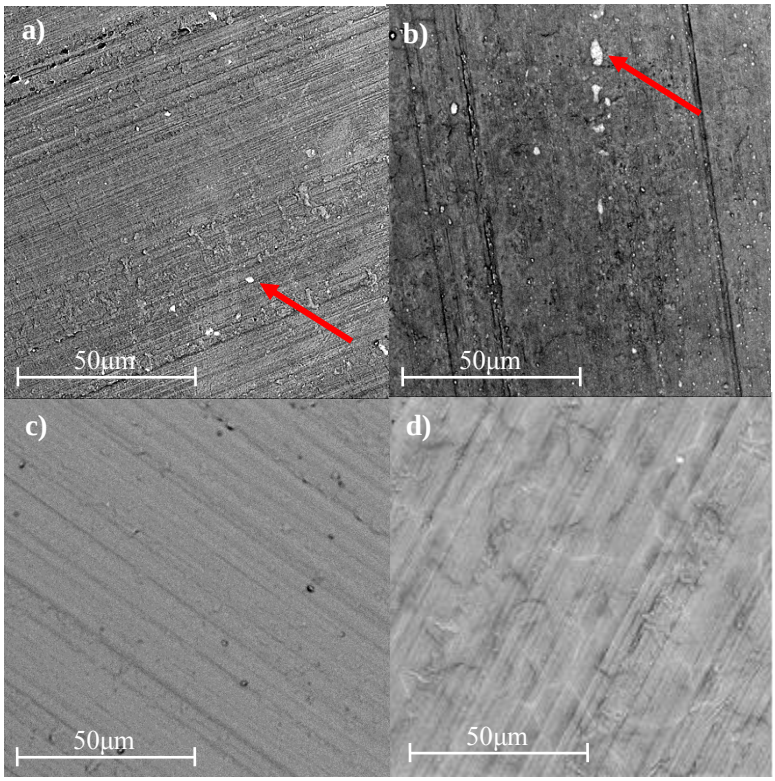

Figure 1. Representative SEM images of a) 15wt% FC, b) 15wt% SC, c) 0wt% FC, d) 0wt% SC films as a function of GNP content and cooling rate (fast cooled, FC or slow cooled, SC).

3.2 Crystallinity

The percent crystallinity, χ, was calculated for each film using the initial heating cycle melting endotherm and cold crystallization exotherm from the DSC data and results are shown in Table 1. (The initial heating cycle was used to reflect the particular processing conditions and thermal history of the samples.) The following equation was then used to calculate χ:

$$\chi = \left\{ \frac{\Delta H_m + \Delta H_c}{\Delta H_m^{\circ}\left(1 - \frac{wt\%}{100}\right)} \right\} \times 100 \qquad (1)$$

χ is the percent crystallinity, ΔH_m is the melting enthalpy of the sample, ΔH_c (< 0) is the cold crystallization enthalpy of the sample, ΔH°_m is the melting enthalpy of 100% crystalline PLA, 93 J/g [8, 9], and wt% is the weight percent of filler in the composite.

Sample ID	T_g [°C]	$T_{m,1}$ [°C]	$T_{m,2}$ [°C]	χ [%]
As received pellets	61.2 ± 0.4	150.0 ± 0.0	-	35.9 ± 0.4
0wt% FC	58.4 ± 0.4	148.1 ± 0.1	153.9 ± 0.1	0.8 ± 0.8
0wt% SC	61.1 ± 0.3	149.1 ± 0.2	153.9 ± 0.0	37.5 ± 1.6
1wt% FC	58.3 ± 0.2	148.1 ± 0.2	153.7 ± 0.0	0.2 ± 0.3
1wt% SC	60.5 ± 0.3	148.5 ± 0.3	153.6 ± 0.1	37.8 ± 1.0
5wt% FC	58.3 ± 0.3	146.6 ± 0.1	153.7 ± 0.1	0.8 ± 0.5
5wt% SC	60.7 ± 0.4	150.8 ± 0.0	-	39.0 ± 1.2
10wt% FC	59.6 ± 0.2	149.4 ± 0.0	153.2 ± 0.6	2.3 ± 0.1
10wt% SC	62.0 ± 0.2	150.3 ± 0.2	-	37.7 ± 0.8
15wt% FC	58.1 ± 0.3	145.5 ± 0.2	153.3 ± 0.1	2.5 ± 0.7
15wt% SC	59.8 ± 0.4	152.2 ± 0.1	-	42.0 ± 0.8

Table 1. Thermal behavior of both the fast cooled (FC) and slow cooled (SC) films as a function of GNP content compared to the as received PLA pellets. (T_g is the glass transition temperature; $T_{m,1}$ is the first melting temperature; $T_{m,2}$ is the second melting temperature; χ is the percent crystallinity)

There is a significant difference in the crystallinity of the fast cooled and slow cooled films. The fast cooled films display a relatively low crystallinity and taking into account standard error, show no significant trend in crystallinity as it relates to GNP concentration. However, the slow cooled films, as expected, displayed a much higher crystallinity than the fast cooled films. (The 15wt% SC film had an increase in crystallinity of over 37% compared to the 15wt% FC film.) When the films are cooled slowly (~0.4°C/min), the polymer chains have higher mobility for a longer period of time allowing for crystalline lamella to form. Also, for the slow cooled films, the crystallinity seems to increase slightly with increased GNP content. (~38% crystallinity for the 0wt% SC sample vs. ~42% crystallinity for the 15wt% SC sample.) GNP and other carbon nanofillers have been shown to act as nucleating agents, promoting crystallization [8, 10]. This slight increase in crystallinity with GNP content could indicate this nucleating effect.

All of the fast cooled samples and some of the slow cooled samples exhibit double melting behavior, which could be indicative of polymorphism or melt-recrystallization phenomena. (Melt-recrystallization is when upon heating original crystals present melt, indicated by the first endotherm, then as heating continues new crystals form and subsequently melt upon continued heating, indicated by the second endotherm [11].) Further investigation of this behavior was explored using WAXD.

PLA has three main polymorphs: α, β, and γ [12]. α is the primary and most common (and stable) crystal form present in PLA [12-14]. β and γ phases are similar and formed under specific thermal and mechanical conditions [12, 13]. The WAXD showed no evidence of polymorphism. All of the peaks obtained were indicative of the primary α form. Furthermore, the crystal structure for both the fast and slow cooled films showed no significant changes with the addition of GNP. The double melting behavior seems to be due to melt-recrystallization.

3.3 Mechanical Behavior

The mechanical behavior was examined and compared for the fast and slow cooled films. As shown in Table 2, the elastic modulus (E) increases with increased GNP content. The stiffening

of the films with increased GNP content is indicative of the polymer chain's hindered mobility caused by the incorporation of GNP in the PLA matrix [15, 16]. Furthermore, the slow cooled films showed a much higher E than the fast cooled films at the same GNP concentration. This is due to the higher crystallinity of the slow cooled films causing the stiffness to increase.

Sample ID	E [MPa]
0wt% FC	2516 ± 72
0wt% SC	3179 ± 54
1wt% FC	2777 ± 73
1wt% SC	3231 ± 65
5wt% FC	2733 ± 27
5wt% SC	3463 ± 45
10wt% FC	2985 ± 80
10wt% SC	3910 ± 13
15wt% FC	3374 ± 319
15wt% SC	3854 ± 33

Table 2. Elastic modulus (E) of the fast cooled (FC) and slow cooled (SC) films as a function of GNP content.

3.4 Electrical Conductivity

The electrical conductivity of the 15wt% FC and 15wt% SC films was examined in order to investigate the effect of cooling rate on the composite conductivity using impedance spectroscopy. Impedance spectroscopy measures the current (I), voltage (V), and phase angle (θ) over a wide range of frequencies [7]. The results indicated that the electrical conductivity of the slow cooled sample (15wt% SC) was higher for both the through-plane and in-plane directions compared to the fast cooled sample (15wt% FC) of the sample GNP concentration. This indicates that there is a correlation between crystal structure and/or degree of crystallinity and electrical conductivity [17], which is in agreement with previous research. The specific mechanism for the higher conductivity in the slow cooled sample for this materials system is currently being investigated.

4. Conclusion

The rate of cooling during compression molding significantly affects the degree of crystallinity of the resultant composite. The slow cooled films were highly crystalline and displayed higher electrical conductivity at the same GNP concentration compared to the fast cooled films which were almost amorphous and displayed lower conductivity. The tensile tests indicate that the composite films stiffen as the GNP content is increased, as well as, an increased stiffness of the slow cooled films compared to the fast cooled films. This indicates hindered mobility of the polymer chains due to the presence of GNP, as well as, decreased mobility of the crystalline lamella. This study indicates a direct correlation between the polymer processing/crystallinity and the overall properties of the resultant films. This will allow us to engineer composite properties such as, electrical conductivity and elastic modulus, by tuning the processing conditions.

Acknowledgements

The author Erin Sullivan would like to acknowledge and thank financial support from the doctoral fellowship from Cytec Engineered Materials (July 2012-June 2014) and the research fellowship from the Georgia Tech Manufacturing Institute (January 2012-present).

References

[1] P. Gonnet, S. Y. Liang, E. S. Choi, R. S. Kadambala, C. Zhang, J. S. Brooks, B. Wang, and L. Kramer. *Current Applied Physics,* 6(1):119-122, 2006.

[2] Q. F. Cheng, J. W. Bao, J. Park, Z. Y. Liang, C. Zhang, and B. Wang. *Advanced Functional Materials,* 19(20):3219-3225, 2009.

[3] A. M. Diez-Pascual, J. W. Guan, B. Simard, and M. A. Gomez-Fatou. *Composites Part a-Applied Science and Manufacturing,* 43(6):997-1006, 2012.

[4] K. Kalaitzidou, H. Fukushima, and L. T. Drzal. *Carbon,* 45(7):1446-1452, 2007.

[5] J. K. Duan, S. X. Shao, L. Ya, L. F. Wang, P. K. Jiang, and B. P. Liu. *Iranian Polymer Journal,* 21(2):109-120, 2012.

[6] A. M. Pinto, J. Cabral, D. A. P. Tanaka, A. M. Mendes, and F. D. Magalhaes. *Polymer International,* 62(1):33-40, 2013.

[7] R. Q. Ou, S. Gupta, C. A. Parker, and R. A. Gerhardt. *Journal of Physical Chemistry B,* 110(45):22365-22373, 2006.

[8] M. Murariu, A. L. Dechief, L. Bonnaud, Y. Paint, A. Gallos, G. Fontaine, S. Bourbigot, and P. Dubois. *Polymer Degradation and Stability,* 95(5):889-900, 2010.

[9] S. S. Ray, K. Yamada, M. Okamoto, Y. Fujimoto, A. Ogami, and K. Ueda. *Polymer,* 44(21):6633-6646, 2003.

[10] K. Fukushima, M. Murariu, G. Camino, and P. Dubois. *Polymer Degradation and Stability,* 95(6):1063-1076, 2010.

[11] M. Yasuniwa, S. Tsubakihara, Y. Sugimoto, and C. Nakafuku. *Journal of Polymer Science Part B-Polymer Physics,* 42(1):25-32, 2004.

[12] X. L. Chen, J. Kalish, and S. L. Hsu. *Journal of Polymer Science Part B-Polymer Physics,* 49(20):1446-1454, 2011.

[13] J. S. Hebert, P. Wood-Adams, M. C. Heuzey, C. Dubois, and J. Brisson. *Journal of Polymer Science Part B-Polymer Physics,* 51(6):430-440, 2013.

[14] W. Hoogsteen, A. R. Postema, A. J. Pennings, G. Tenbrinke, and P. Zugenmaier. *Macromolecules,* 23(2):634-642, 1990.

[15] Z. Jin, K. P. Pramoda, G. Xu, and S. H. Goh. *Chemical Physics Letters,* 337(1-3):43-47, 2001.

[16] A. M. Diez-Pascual, J. W. Guan, B. Simard, and M. A. Gomez-Fatou. *Composites Part a-Applied Science and Manufacturing,* 43(6):1007-1015, 2012.

[17] K. Kalaitzidou, H. Fukushima, and L. T. Drzal. *Materials,* 3(2):1089-1103, 2010.